36th EPS Conference on Plasma Phys. Sofia, June 29 - July 3, 2009 ECA Vol.**33E**, P-4.051 (2009)

Wavelet Analysis of 2D Turbulence in a Non-neutral Plasma

M. Romé, G. Bettega, R. Pozzoli

I.N.F.N. Sezione di Milano and Dipartimento di Fisica, Università degli Studi di Milano, Italy

Highly magnetized pure electron plasmas confined in Malmberg-Penning traps allow to perform experiments on quasi-ideal two-dimensional (2D) fluid dynamics. In fact, under typical experimental conditions the transverse dynamics of the electron plasma is well described by the drift-Poisson system [1] (cold non-relativistic guiding center approximation)

$$\partial n/\partial t + \mathbf{v}\cdot\nabla n = 0, \quad \mathbf{v} = -\nabla\phi\times\mathbf{e}_z/B, \quad \nabla^2\phi = en/\varepsilon_0 \tag{1}$$

where n is the plasma density, ϕ the electrostatic potential, B the magnetic field, $\mathbf{v}$ the velocity field, $-e$ the electron charge, ε_0 the vacuum permittivity, and $\mathbf{e}_z$ the unit vector in the axial direction. Eqs. (1) are isomorphic to the Euler equations for an ideal (incompressible, inviscid) fluid, with vorticity $\zeta = en/\varepsilon_0$ and stream function $\psi = \phi/B$. In the electron plasma case, no boundary layer exists, free slip boundary conditions hold, the velocity field is divergence free and viscosity effects (mainly due to collisions of the electrons with the residual neutral gas) become negligible under ultra high vacuum conditions (residual gas pressure p of the order of a few 10^{-9} mbar), so that effective Reynolds numbers up to $\approx 10^5$ can easily be reached [2].

The classical treatments of 2D isotropic and homogeneous turbulence [3] strongly rely on the use of the Fourier representation. On the other hand, in a 2D turbulent fluid long-lived coherent structures with different spatial scales develop even at very high Reynolds numbers, breaking the homogeneity hypothesis. Wavelet transforms, which have well localized basis functions both in physical and "wave-number" space [4], are best suited to discriminate the coherent and the incoherent parts of the flow. A preliminary comparison of Fourier and wavelet analysis applied to experimental data of turbulent electron plasmas was described in Ref. [5]. Recently, a wavelet analysis identifying the coherent and the incoherent parts of the flow has been reported [6].

The experimental data reported here have been obtained in the Malmberg-Penning trap EL-TRAP [7, 8] (see Fig. 1). The device operates according to an injection-hold-dump cycle. A high resolution CCD camera records the light produced on a phosphor screen collecting the particles ejected from the device when the potential barrier is removed. The image on the screen represents the axially averaged plasma density distribution. Several machine cycles are repeated keeping the injection parameters fixed (with a very high shot-to-shot reproducibility) and increasing the trapping time.

An example of time evolution of the plasma is shown in Fig. 2. The first frame reflects the

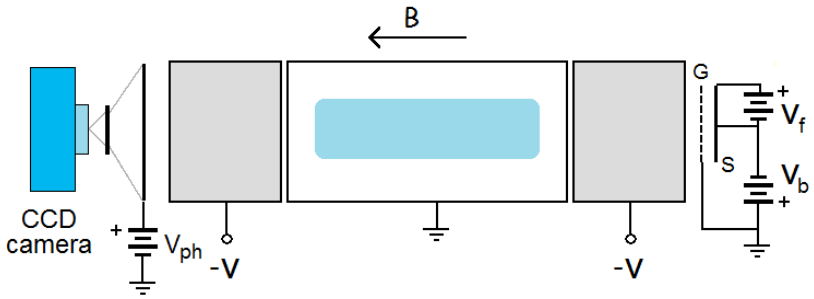

Figure 1: Schematic of the Malmberg-Penning trap ELTRAP [7]. The electrons are generated by a thermionic cathode (S) heated with a constant current and negatively biased with respect to a grounded grid (G). A low density ($n \simeq 10^{12} - 10^{13}$ m^{-3}) and temperature (few eV) plasma is contained within a stack of hollow cylindrical electrodes with radius 4.5 cm. The electrons are trapped axially by two negative voltages $-V$, and radially by an axial magnetic field B. In the experiments the plasma length is $\simeq 50$ cm, $B = 0.167$ T and $p \simeq 5 \times 10^{-9}$ mbar.

shape of the spiral thermionic cathode used for the injection of the electrons. The diocotron instability [1] rapidly leads to a highly non-linear evolution of the flow. Several small vortices form, which then interact through close encounters resulting in merger events and emission of vorticity filaments, and leading eventually to the formation of a diffuse background.

The evolution of the flow is studied with a wavelet (Symlet8) multiresolution analysis, which successively decomposes the 2D vorticity (density) field into coefficients that contain coarse and fine details at increasing resolution. In order to separate the coherent and the incoherent part of the flow, an adaptive threshold is applied [9]. The coherent flow $\zeta_>$ is reconstructed using only a small fraction of the wavelet coefficients ($\simeq 1.1\%$) but it contains the greatest part (99.3%) of the total enstrophy. On the contrary, the incoherent flow $\zeta_<$ is described by the major part of the wavelet coefficients but it contains a very small fraction of the enstrophy [8].

The spectral analysis (see Fig. 3) evidences that most of the enstrophy is contained at the bigger spatial scales. This fact is consistent with the observation of the vorticity (density) fields and the persistence of large amplitude vortices. Note that although enstrophy and all higher moments of vorticity are conserved by the 2D Euler equations, their measured values generally decrease with time due to coarse-graining [2], so that the $\zeta_>(k)$ curves turn out to be successively lower. The incoherent field contains negligible enstrophy at large scales and represents the dominant contribution to the enstrophy at large k. Different scaling regions appear in the spectrum. The first change of the slope is found to be related with the maximum enstrophy of the coherent part at the corresponding scale, which in turn is linked to the presence of the

dominating coherent structures. Namely, Fig. 4 shows the spatial distribution of the enstrophy at different scales for a trapping time $\tau = 2$ μs. The maximum content of enstrophy is found in plot (b), corresponding to a scale length of approximately 5 mm or to a spatial wave-number $k \sim 300$ m^{-1}, i.e., around the position of the maximum of $\zeta_>(k)$ in Fig. 3.

The two spectra $\zeta_>(k)$ and $\zeta_<(k)$ show quite different scaling laws in the intermediate range $10^3 < k < 10^4$ m^{-1}, i.e., $\zeta_>(k) \propto k^{-1}$ while $\zeta_<(k) \propto k^2$. These scalings are consistent, e.g., with those found in Ref. [10]. The presence of localized coherent structures in the flow introduces nonnegligible contributions at all scales (wave-numbers) in the Fourier space, and the wavelet spectra do not reproduce the classical results of Kraichnan and Batchelor [3] obtained for a 2D homogeneous and isotropic turbulence.

The results of the wavelet-based separation of the flow into two dynamically different components appear to be in qualitative agreement with numerical simulations of 2D turbulence [9], and support the hypothesis that the computational complexity of turbulent flows could be reduced in simulations by considering only coherent structures interacting with a statistically modeled incoherent background.

This work was supported by the Italian Ministry for University and Scientific Research 'PRIN-2007' funds.

References

[1] R. H. Levy, Phys. Fluids **8**, 1288 (1965)

[2] D. A. Schecter, D. H. E. Dubin, K. S. Fine and C. F. Driscoll, Phys. Fluids **11**, 4162 (1999)

[3] R. H. Kraichnan and D. Montgomery, Rep. Prog. Phys. **43**, 547 (1980)

[4] S. G. Mallat, *A wavelet tour of signal processing* (Academic Press, U.S.A., 1999)

[5] G. Bettega, F. Cavaliere, M. Cavenago, F. De Luca, R. Pozzoli and M. Romé, Proc. 34th EPS Conference on Plasma Physics (Warsaw, Poland, 2007), ECA Vol 31F, P-2.099

[6] Y. Kawai and Y. Kiwamoto, Phys. Rev. E **78**, 036401 (2008)

[7] M. Amoretti, G. Bettega, F. Cavaliere, M. Cavenago, F. De Luca, R. Pozzoli and M. Romé, Rev. Sci. Instrum. **74**, 3991 (2003)

[8] G. Bettega, R. Pozzoli and M. Romé, New J. Phys. **11**, 053006 (2009)

[9] M. Farge, K. Schneider and N. Kevlahan, Phys. Fluids **11**, 2187 (1999)

[10] K. Schneider, M. Farge, A. Azzalini and J. Ziuber, J. Turbul. **7**, N44 (2006)

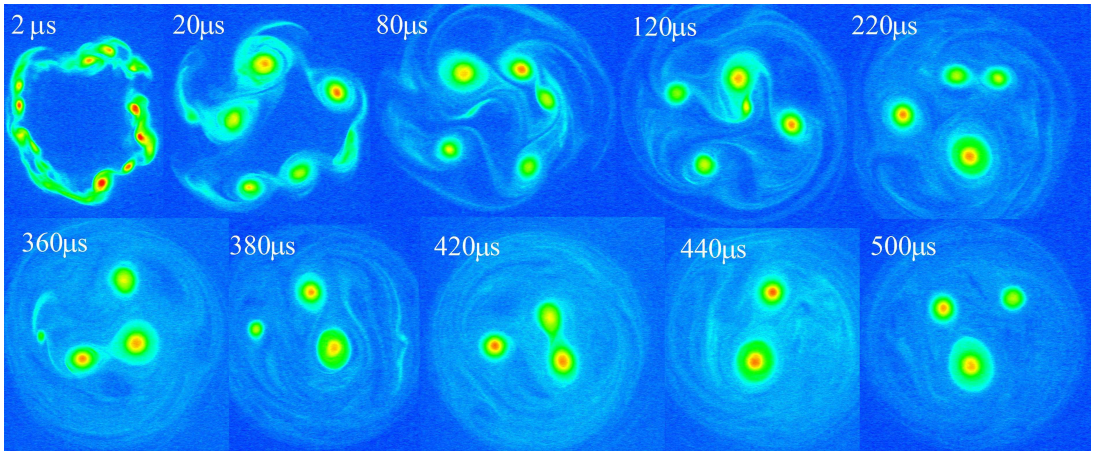

Figure 2: Time evolution of the plasma (the trapping time is indicated at the top left corner of each frame).

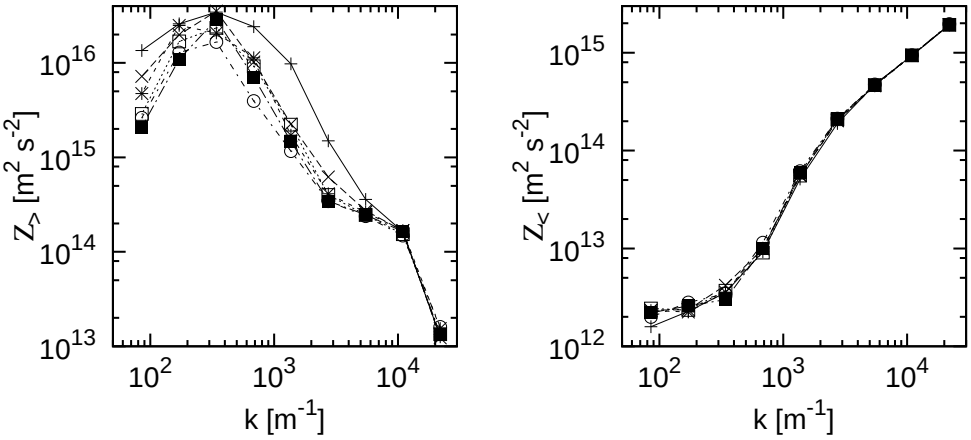

Figure 3: Spectral enstrophy distribution of the coherent flow (left) and of the incoherent flow (right) for $\tau = 2$ μs (plus symbols), 20 μs (crosses), 40 μs (asterisks), 80 μs (open squares) and 200 μs (full squares).

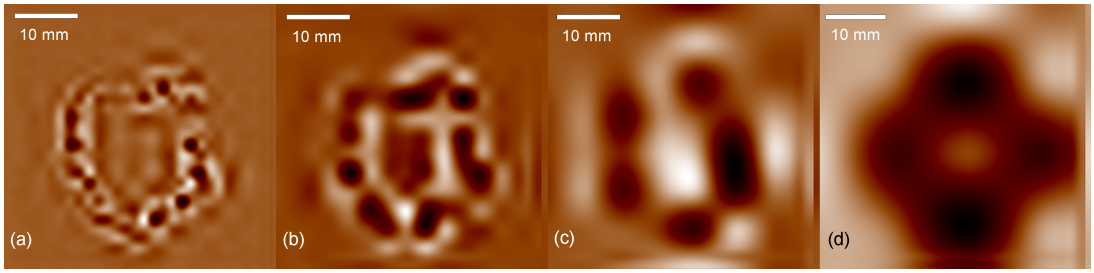

Figure 4: Spatial distribution of the enstrophy at different scales for $\tau = 2$ μs (see Fig. 2), using an inverted color palette. The panels correspond to a scale of 256, 128, 64 and 32 pixels of the original image, respectively.